

Stable icosahedral nanoparticles in an as-grown Au–Fe alloy

D.K. Saha^a, K. Koga^{b,c}, and H. Takeo^b

National Institute for Advanced Interdisciplinary Research, Tsukuba, Ibaraki 305-8562, Japan

Received: 1 September 1998 / Received in final form: 10 November 1998

Abstract. The morphologies of Au–Fe alloy nanoparticles with an 11% Fe mean atomic concentration were investigated by means of high-resolution electron microscopy. The icosahedral morphology was very frequently found in the particles that were generated by the vapor condensation method with helium and deposited on an amorphous carbon film. A high fraction of the icosahedral morphology still remained even after the supported particles were annealed at 723 K for 1 h in a vacuum; this suggests the minimum-energy structure for the alloy particles is icosahedral. As for the low production rate of the icosahedral morphology in the pure Au particles produced under the same conditions, the present results indicate that the icosahedral form is stabilized by the addition of Fe atoms into the Au particles.

PACS. 61.46.+w Clusters, nanoparticles, and nanocrystalline materials – 61.16.Bg Transmission, reflection and scanning electron microscopy – 61.66.Dk Alloys

In recent years, the structure and stability of metallic nanoparticles in the size range of 1–10 nm in diameter have attracted much attention, since their structures are reported to be different from bulk crystal structures. Nanoparticles made from a single element, e.g., Au, Ag, etc., often show multiply-twinned decahedral (DH) and icosahedral (IH) structures which do not obey the crystallographic symmetry rules [1–3]. Generally the structure of as-grown nanoparticles appears to be a mixture of different morphologies at small size. However, it has been observed as an exceptional case that the gas-phase-grown Au predominantly exhibits decahedral structure [4]. In the present work, our interest is what will happen to the structure when a second element (Fe) is introduced into the Au particle.

The technique used to form and deposit nanoparticles involves vaporization from an alloy ingot, the formation of particles in the helium gas stream, and deposition on the amorphous carbon film. The alloy particles were generated under the conditions of carbon crucible temperature 1623 K, helium gas flow rate 10 atm·l/min, and pressure for production 2.9 kPa. Details of the apparatus have been described elsewhere [5, 6]. The Au–Fe alloy particles with 2–10 nm diameter and a mean Fe atomic concentration of 11% were generated from an Au–20%–Fe alloy ingot, and deposited sparsely on an amorphous carbon film. The concentration difference between the particles and the source is due to the difference in vapor pressures

of the two elements. The mean concentration of the particles was determined with $\pm 3\%$ accuracy by the energy-dispersive spectroscopic measurement of a thick deposit on an Si wafer.

The high-resolution electron microscopy (HREM) observations for the as-grown particles were performed using a Jeol JEM-2010 electron microscope with 200 kV electron accelerating voltage, 0.194 nm point-to-point resolution, 0.8 mrad beam divergence and $C_s = 0.5$ mm. To examine the stability of the as-grown particles, we annealed them at 723 K for 1 h, using a halogen lamp irradiation under vacuum just after deposition, then slowly cooled them down to room temperature for 5 h. The annealing temperature was selected experimentally to be the maximum temperature for the amorphous carbon film above which the film was broken. The structural observations for the annealed particles were also performed by HREM.

The upper part of Fig. 1 shows a HREM picture of the as-grown Au–Fe particles on the amorphous carbon film. In this photograph, no crystalline particle can be found, and most of the particles show characteristic symmetrical patterns. We could identify these patterns to be of IH structure along different orientations with a help of a computer simulation. Multi-slice calculations for the HREM images of an IH model particle were carried out in a manner similar to that which Urban *et al.* [7] have employed. The model has 11 geometrical shells with 5083 Au atoms, and its diameter is comparable to that of the observed particles denoted by c, d, f, h and i in Fig. 1. Finally, we could find the images similar to the observed ones among 41 calculated images corresponding to different orientations of the IH structure. The calculated images are shown in the lower part of Fig. 1. The c' image is along the 2-fold axis of the IH structure. The d' image is along a direc-

^a Permanent address: Bangladesh Atomic Energy Commission, Dhaka, Bangladesh

^b Current address: National Institute of Materials and Chemical Research, 1-1 Higashi, Tsukuba, Ibaraki 305-8565, Japan

^c e-mail: kkoga@home.nimc.go.jp

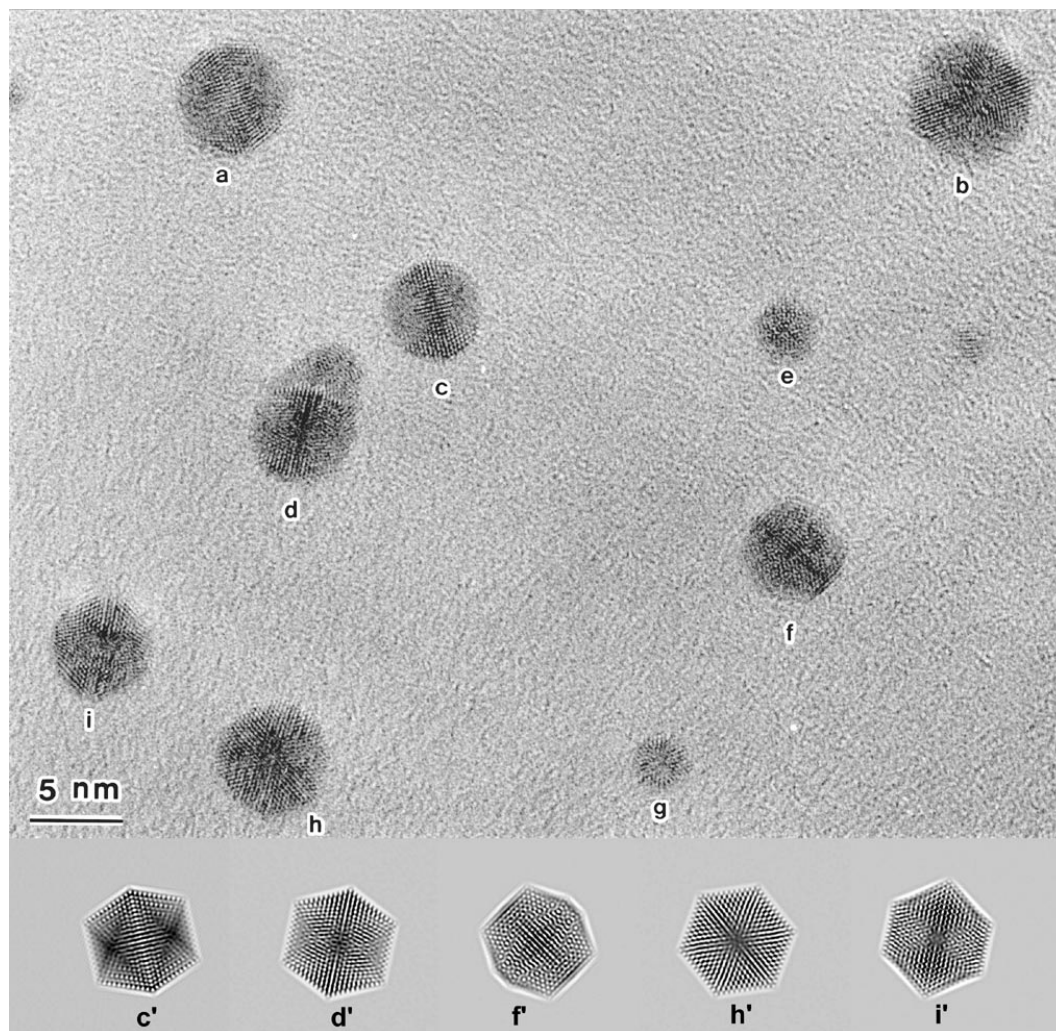


Fig. 1. Upper part: An HREM picture of the as-grown Au-11%-Fe particles deposited on an amorphous carbon film. The internal structures of all particles shown in this picture could be identified to be the icosahedral structure along different orientations. a,c: 2-fold axis; b,d: in between 2- and 3-fold axes; e: nearly 5-fold axis; f: in between 2- and 5-fold axes; g,h: nearly 3-fold axis; i: in between 3- and 5-fold axes. Lower part: Calculated HREM images for an Au icosahedral model structure with 11 geometric shells. c' : 2-fold axis; d' : a direction rotated by 10° from the 2-fold towards the 3-fold axis; f' : a direction rotated by 10° from the 5-fold towards the 2-fold axis; h' : a direction doubly rotated by 2° from the 3-fold towards the 5-fold axis and by 9° towards the 2-fold axis; i' : a direction rotated by 20° from the 5-fold towards the 3-fold axis.

tion in between the 2- and 3-fold axes. The f' image is along a direction in between the 5- and 2-fold axes. The h' image is nearly along the 3-fold axis. The i' image is along a direction in between the 5- and 3-fold axes. These calculated images from the IH structure show a good agreement with the observed images. The observed IH particles show more rounded shapes than the geometrical model. This indicates that the corner atoms are lacking, resulting in reduction of the surface energy. The other particle images, a, b, e, and g, can also be explained with the IH structure. The fractions of IH along different orientations, and DH, crystalline, and unidentified structures for the as-grown sample, are listed in Table 1. The total fraction of IH was found to be about 80% of 182 observed particles. This indicates that the IH structures can be formed with the Au and Fe binary mixture. Although we did not

measure the Fe concentration particle by particle, the predominant IH particles should have about 10% Fe atoms. One more positive proof for the bimetallic particles can be found through positive comparison of the results on the as-grown and annealed Au particles (see below). The predominant particle morphologies of Au are completely different from those of the Au-11%-Fe. This also supports the existence of the bimetallic particles.

The annealed Au-11%-Fe particles also showed the IH structures predominantly. The fractions of IH and the other morphologies are shown in Table 1. The high fraction of IH was not changed by the annealing; this suggests that the IH form is the minimum-energy structure of the Au-11%-Fe nanoparticles. Since the identification of the IH structure in HREM figures can be very difficult when its orientation is shifted far from three particular axes,

Table 1. Fractions of morphologies of icosahedral (IH) along different orientations, decahedral (DH), crystalline, and unidentified structures for both of the as-grown and annealed Au–11%–Fe particles.

morphology	fraction (%)	
	as-grown (total: 182)	annealed (total: 175)
IH (2-fold)	18	10
IH (3-fold)	7	8
IH (5-fold)	8	7
IH (2–3 folds)	26	23
IH (2–5 folds)	12	14
IH (3–5 folds)	7	12
IH (total)	78±7	74±7
DH	1	~0
Crystalline	2	4
Unidentified	19	22

some improperly oriented IH structures might be counted as “unidentified”. Therefore, we can say that the yield of the IH particles generated through gas-phase growing is at least 80%. This indicates a very high production rate for the IH particles. In contrast, DH and crystalline structures were very infrequent, independently of the annealing treatment.

The phase segregation temperature of the Au–11%–Fe bulk alloy is known to be ~ 710 K [8]. The annealing temperature was slightly higher than this temperature. Since we accomplished the long-time annealing for the particles and cooled them very slowly across the segregation line, this procedure certainly induced the phase segregation into two phases of Au and α -Fe in the bulk alloy case. However, the Au–11%–Fe nanoparticles with the IH forms were not destroyed by the annealing, indicating that the bulk phase diagram cannot be applied to the nanometer-sized alloy. A different stabilizing mechanism seems to be working for the nanometer system.

We have previously found a high production rate of the IH form in the Au–25%–Cu alloy particles [9, 10]. In this case, however, as-grown particles showed mostly unidentified complex structures, and the IH form was created by annealing. The reason for the complex as-grown structures in the Au–Cu case is considered to be the lack of formation of stable IH nuclei at the early stage of growing. In the present Au–Fe case, stable IH nuclei were probably created and grown epitaxially, shell by shell.

We have previously carried out the structural analysis for Au particles. Using both an *in-situ* X-ray diffraction technique and HREM, small Au particles 1–3 nm in diameter were found to have predominantly the DH structure [4]. Larger Au particles also showed a large fraction with the DH structure, but a small fraction with the IH structure [9]. After the Au particles were annealed on an amorphous carbon film under the same experimental conditions as in the present alloy case, the IH form still constituted a small fraction [9]. According to recent theoretical calculation, the crystalline forms are the most stable

when the number of atoms in a particle is greater than ~ 200 , i.e., the particle is a few nanometers in diameter, and below this size, the Marks-type DH form becomes stable [11]. On the other hand, the IH form of Au does not take the minimum energy over the whole nanometer-size range [11]. Our experimental result of the low production rate for the IH morphology of Au agrees well with this theoretical result. Considering this fact, the present result of the stable IH form in Au–11%–Fe particles is very surprising. Only the addition of $\sim 10\%$ Fe atoms into the Au particle have changed its stability dramatically. In other words, the minimum-energy form of the Au particle has been modified from crystalline to IH form by the addition of Fe.

The stabilization mechanism of the IH form from the addition of Fe into Au cannot be so simply understood. At the present stage we can not make any conclusions; however, there should be two possibilities: geometrical or electronic effect. The former possibility comes from the IH structure itself. To construct the geometrical IH form, radial interatomic distances lower by 5.1% than tangential distances are required, where both the radial and the tangential distances are constant, independently of the size. Such an atomic arrangement of the geometrical model is not the most stable. The relaxed IH form can be obtained by the calculation [12, 13]. For the high surface energy of this model to be reduced, its flat surfaces have to be convex; the result is that both the radial and tangential distances are changed from the center to the surface, where the distances around the center region are contracted, and those around the surface are dilated. According to the Ni case [13], the difference between the center and the surface distances becomes 7%–8% in an IH particle with 11 shells. This difference is increased with the particle size and, finally, the IH form becomes less stable. When a second element with a smaller atomic radius is introduced in an IH structure, the strain energy can be reduced effectively. The atomic radius of Fe is 86% of that of Au. Such a relaxation mechanism is a candidate for explanation of the present result. However, a molecular dynamics simulation that takes both geometrical and electronical effects into account should be done. Further experiments on the concentration dependence of the stable IH formation are now in progress.

This work was supported in part by the New Energy and Industrial Technology Development Organization (NEDO).

References

1. S. Ino: J. Phys. Soc. Jpn. **21**, 346 (1966)
2. K. Kimoto, I. Nishida: J. Phys. Soc. Jpn. **22**, 940 (1967)
3. C. Altenhein, S. Giorgio, J. Urban, K. Weiss: Z. Phys. D **19**, 303 (1991)
4. K. Koga, H. Takeo, T. Ikeda, K. Ohshima: Phys. Rev. B **57**, 4053 (1998)

5. K. Koga, H. Takeo: *Rev. Sci. Instrum.* **67**, 4092 (1996)
6. K. Koga, T. Ikeda, K. Ohshima, H. Takeo: *Jpn. J. Appl. Phys.* **36**, 7050 (1997)
7. J. Urban, H. Sack-Kongehl, K. Weiss: *Z. Phys. D* **28**, 247 (1993)
8. T.B. Massalski: *Binary Alloy Phase Diagram* (American Society for Metals, Metal Parks, OH 1986)
9. K. Koga, D.K. Saha, H. Takeo: in *Proceedings of the International Conference on Similarities and Differences between Atomic Nuclei and Clusters*, Tsukuba, Japan, 1997, ed. by Y. Abe, I. Arai, S.M. Lee, K. Yabana (AIP conference proceedings 416) p. 431
10. D.K. Saha, K. Koga, H. Takeo: *Nanostruct. Mater.* **8**, 1139 (1997)
11. C.L. Cleveland, U. Landman, M.N. Shafiqullin, P.W. Stephens, R.L. Whetten: *Z. Phys. D* **40**, 503 (1997)
12. J. Farges, M.F. de Feraudy, B. Raoult, G. Torchet: *Acta Cryst. A* **38**, 656 (1982)
13. C.L. Cleveland, U. Landman: *J. Chem. Phys.* **94**, 7376 (1991)